Two-Body Bound States & The Bethe-Salpeter Equation

, M. Pichowsky*, M. Kennedy†, M. Strickland‡

January 18, 1995

Abstract

he Bethe-Salpeter formalism is used to study two-body bound states within a scalar theory: two scalar fields interacting via the exchange of a third massless scalar field. The Schwinger-Dyson equation is derived using functional and diagrammatic techniques, and the Bethe-Salpeter equation is obtained in an analagous way, showing it to be a two-particle generalization of the Schwinger-Dyson equation. We also present a numerical method for solving the Bethe-Salpeter equation without three-dimensional reduction. The ground and first excited state masses and wavefunctions are computed within the ladder approximation and space-like form factors are calculated.

The authors: Mike, Melissa, and Mike.

*pichowsk@theory.phy.anl.gov; Physics Division, Argonne National Laboratory, Argonne, IL 60439-4843
†mlk@curie.unh.edu; Physics Department, University of New Hampshire, Durham, NH 03824
‡strickla@phy.duke.edu; Duke University, Durham, NC 27706

1 Introduction

Many of the bound systems that occur in nature, most notably the low lying hadronic states, are comprised of highly relativistic particles. Thus, an approach to study bound states within the formalism of Quantum Field Theory (QFT), is clearly desirable. In this paper we investigate the two-body bound state, using the scattering matrix M as our starting point. Typically one calculates the scattering matrix by the use of perturbation theory. That is, the scattering matrix M is expanded in powers of the coupling constant and only terms of low order are retained. However, it is well known that perturbation theory can *never* generate a bound state [1]. This is because the formation of a bound state is accompanied by the appearance of a pole in the scattering matrix, and any finite sum of perturbative graphs can never create such a pole. On the other hand, the required pole may be generated if one sums over an *infinite* subset of graphs. In 1951, E. E. Salpeter and H. A. Bethe introduced a means of achieving this as an alternative to a perturbative expansion [2]. Within the Bethe-Salpeter formalism, the scattering matrix M is given by an integral equation of the form $M(p) = V(p) + \int \mathrm{d}k\, F(p,k)M(k)$. The effect of the integral equation is to sum the contribution due to *all* powers of the interactions contained in $F(p,k)$, not just some finite number.

Solving the Bethe-Salpeter equation is made difficult by the presence of various poles along the integration contours. The study of these poles was pioneered by Wick and Cutkosky in 1954, who suggested performing an analytic continuation into Euclidean space (a Wick rotation) to avoid the troublesome poles [3] . However, it has recently been suggested that one might be suspicious of performing an analytic continuation to Euclidean space as discussed by Wick and Cutkosky on account of poles in the complex plane of the fermion propagator [4]. One must take care to include the contributions of these poles which may not be a trivial matter.

Alternatives to performing a Wick rotation have since been introduced, one of which handles the difficulty with poles along integration contours by replacing the four dimensional Bethe-Salpeter kernel by an effective three dimensional kernel. This is referred to as a *three dimensional reduction* [5]. The resulting integral equation is similar in form to the Lippman-Schwinger equation of non-relativistic quantum mechanics and so does not treat time and space on the same footing.

In this paper, we will refrain from performing a three dimensional reduction in favor of working in Euclidean space. We would like to investigate whether the Bethe-Salpeter equation in Euclidean space affords reasonable solutions before we resort to performing a three dimensional reduction.

We assume that one *is* allowed to formulate an action for QFT in Euclidean space. The validity of this assumption is beyond the scope of this work. However, inspired by the recent successes of phenomenological Schwinger-Dyson approaches, Lattice QCD calculations, as well as some Quantum Gravity theories [4], we proceed to work in Euclidean space.

This paper is divided into two main sections. In the first, we derive the Bethe-Salpeter equation for a scalar Yukawa-like Lagrangian and point out its connection to other integral field equations such as the Schwinger-Dyson equation. We also derive the Bethe-Salpeter kernel within the so-called "ladder approximation" from an effective action. Since analytic solution of the Bethe-Salpeter equation is generally not possible, we outline a numerical method for solving the equation by an iterative technique. We determine the vertex function for the ground and first excited states and compute the ground state form factor of our model Lagrangian.

2 Functional Derivation of Field Equations

We would like to go through the derivation of the Bethe-Salpeter equation, starting from a model Lagrangian and using the path integral formalism in Euclidean space. (Another functional approach using composite field operators is outlined in Appendix B). Appendix A outlines how to transform a Minkowski space Lagrangian to Euclidean space. We study a model with two scalar particles ϕ_1 and ϕ_2 exchanging a third scalar particle Φ. Within the path integral formalism, the partition function or generating functional Z for this theory is given by

$$Z[j_1, j_2, J] = \int \mathcal{D}(\phi_1, \phi_2, \Phi)\, e^{-S}, \tag{2.1}$$

where

$$S = \int \mathrm{d}^4x \left(\mathcal{L} - \sum_{i=1}^{2} j_i \phi_i - J\Phi \right) \tag{2.2}$$

$$\mathcal{L} = \frac{1}{2} \sum_{i=1}^{2} \left(\partial_\mu \phi_i \partial_\mu \phi_i + m_i^2 \phi_i^2 \right) + \frac{1}{2} \left(\partial_\mu \Phi \partial_\mu \Phi + M^2 \Phi^2 \right) + \frac{g}{2} \left(\phi_1^2 \Phi + \phi_2^2 \Phi \right). \tag{2.3}$$

Here we can see the first advantage of going into Euclidean space. The integrand in (2.1) is negative definite, so it clearly converges. In Minkowski space an $i\epsilon$ term must be added to the integrand to ensure convergence.

2.1 Klein-Gordon Equation with Self-Energy Contribution

Before we jump immediately into the Bethe-Salpeter equation, it is useful to see how to derive other field equations from the generating functional. Field equations arise from the observation that path integrals of functional derivatives vanish (if the integrand vanishes for large values of the fields). This is fishy in the Minkowski representation of the generating functional since the i causes the integrand to oscillate, but in the Euclidean representation the integrand now has an exponentially decreasing form, and therefore satisfies the boundary condition. To get the Klein-Gordon equation we simply evaluate

$$\int \mathcal{D}(\phi_1, \phi_2, \Phi)\, \frac{\delta e^{-S}}{\delta \phi_{1,2}(x)} = 0. \tag{2.4}$$

For example, consider the functional derivative with respect to ϕ_1:

$$\int \mathcal{D}(\phi_1, \phi_2, \Phi)\, \frac{\delta e^{-S}}{\delta \phi_1(x)} = \int \mathcal{D}(\phi_1, \phi_2, \Phi)\, \left(\partial_\mu \partial_\mu \phi_1(x) - m_1^2 \phi_1(x) - g\phi_1(x)\Phi(x) + j_1(x) \right) e^{-S} = 0, \tag{2.5}$$

where we have performed an integration by parts on the derivative term to get both derivatives acting on one ϕ_1. We can write this as a functional differential equation by making the substitutions $\phi_1(x) \to \delta/\delta j_1(x)$ and $\Phi(x) \to \delta/\delta J(x)$ [1]

$$\left[-\partial_\mu\partial_\mu + m_1^2 + g\frac{\delta}{\delta J(x)}\right]\frac{\delta Z(j_1, j_2, J)}{\delta j_1(x)} = j_1(x)Z[j_1, j_2, J]. \tag{2.6}$$

To get things in terms of the two-particle Green's function we take another derivative – this time with respect to $j_1(y)$ – and turn off the sources for particles one and two ($j_1(x) = j_2(x) = 0$). Remembering that the two point Schwinger function (in the presence of a third particle source J) is given by

$$G_1(x, y; J) = \frac{\int\mathcal{D}(\phi_1, \phi_2, \Phi)\, \phi_1(x)\phi_1(y)\, e^{-S|_{j_1=j_2=0}}}{\int\mathcal{D}(\phi_1, \phi_2, \Phi)\, e^{-S|_{j_1=j_2=0}}} = \left(\frac{\delta^2 Z[j_1, j_2, J]}{\delta j_1(x)\delta j_1(y)}\right)_{j_1=j_2=0} Z^{-1}[0, 0, J]. \tag{2.7}$$

We apply the derivative operator $\delta/\delta j_1(y)$ to (2.6) giving

$$\left(\left[-\partial_\mu\partial_\mu + m_1^2 + g\frac{\delta}{\delta J(x)}\right] G_1(x, y; J)Z[J]\right)_{j_1=j_2=0} = \delta^4(x-y)Z[J]. \tag{2.8}$$

Expanding the functional derivative on the end, and multiplying the whole equation by $Z^{-1}[J]$ gives

$$\left(\left[-\partial_\mu\partial_\mu + m_1^2 - g\langle\Phi(x, J)\rangle + g\frac{\delta}{\delta J(x)}\right] G_1(x, y; J)\right)_{j_1=j_2=0} = \delta^4(x-y), \tag{2.9}$$

with

$$\langle\Phi(x, J)\rangle \equiv Z^{-1}[J]\frac{\delta}{\delta J(x)}Z[J]. \tag{2.10}$$

In the limit that $J \to 0$, $\langle\Phi\rangle$ goes to zero[2] leaving

$$\left(\left[-\partial_\mu\partial_\mu + m_1^2 + g\frac{\delta}{\delta J(x)}\right] G_1(x, y; J)\right)_{j_1=j_2=J=0} = \delta^4(x-y). \tag{2.11}$$

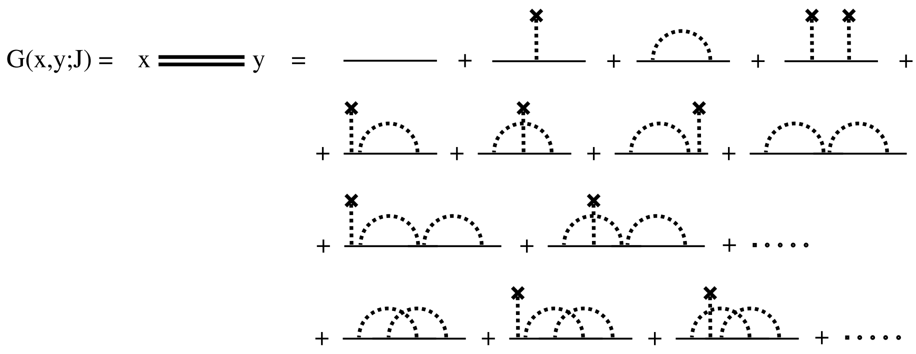

Figure 1. Diagrammatic expansion of G_1. Solid and dotted lines are ϕ_1 and Φ propagators respectively, and $\times$ stands for a source J.

In the following section we will evaluate the functional derivative of G_1 with respect to J and see what this corresponds to, but first we would like to show how to determine its structure graphically. Consider the diagrammatic expansion of $G_1(x, y; J)$ as shown in Figure 1. To take the functional derivative with respect to $J(x)$ we simply take one of the J lines from each graph and attach them to the point x, and then set $J = 0$. This eliminates any graph with more than one source interaction.

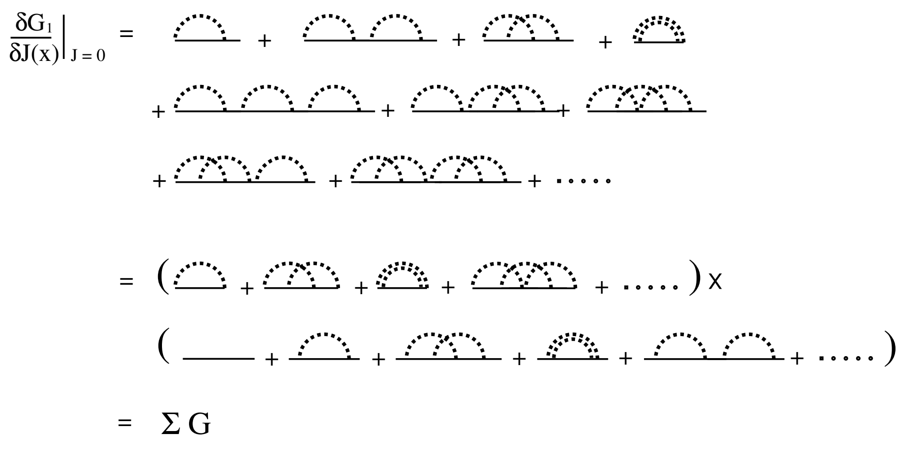

Figure 2. (a) Functional derivative of G with respect to J. (b) Factorization of (a) into self-energy and Green's function.

Looking at this expansion we see that the functional derivative with respect to $J(x)$ generates the self-energy terms! This is an important realization which reappears in our analysis of the Bethe-Salpeter equation. There we will see that a functional derivative of the four-point function with respect to external sources will generate the two-particle irreducible kernel.

To derive the factorization of the last term in (2.11) more formally, we have to investigate the structure of the functional derivative of $G_1(x,y;J)$ with respect to J . To take the functional derivative we use the following identity: (the chain rule for functional derivatives)

$$\frac{\delta}{\delta J(x)} = \int \mathrm{d}^4 z \, \frac{\delta\langle\Phi(z)\rangle}{\delta J(x)} \frac{\delta}{\delta\langle\Phi(z)\rangle} = \int \mathrm{d}^4 z \; \Delta_\Phi(x,z) \frac{\delta}{\delta\langle\Phi(z)\rangle}, \tag{2.12}$$

where $\Delta_\Phi(x,z)$ is the propagator for Φ^3. To evaluate the functional derivative of G_1 with respect to $\langle\Phi\rangle$ we make use of the fact that $G_1(x,y)$ has an inverse which is obtainable by Legendre transformation [6]

$$G_1(x,y) = \left(\frac{\delta^2 \Gamma_1}{\delta\phi_1(x)\delta\phi_1(y)} \right)^{-1} \equiv \Gamma_1^{-1}(x,y). \tag{2.13}$$

Derivatives of inverses can be calculated using the identity

$$\frac{\delta\left(\Gamma_1 \Gamma_1^{-1}\right)}{\delta\langle\Phi(z)\rangle} = 0, \tag{2.14}$$

which gives

$$\frac{\delta\Gamma_1^{-1}(x,y)}{\delta\langle\Phi(z)\rangle} = -\int \mathrm{d}^4 z_1 \int \mathrm{d}^4 z_2 \; G_1(x,z_1) \frac{\delta\Gamma_1(z_1,z_2)}{\delta\langle\Phi(z)\rangle} G_1(z_2,y). \tag{2.15}$$

This is particularly nice since the functional derivative of Γ_1 with respect to $\langle\Phi(z)\rangle$ has a nice "physical" interpretation

$$\frac{\delta\Gamma_1(z_1,z_2)}{\delta\langle\Phi(z)\rangle} = \frac{\delta}{\delta\langle\Phi(z)\rangle} \frac{\delta^2\Gamma}{\delta\phi_1(z_1)\delta\phi_1(z_2)} \equiv g\Lambda_1(z;z_1,z_2), \tag{2.16}$$

where Λ_1 is the connected, irreducible vertex function for our theory [7]. Therefore, this functional derivative just returns all of the possible vertices that can be constructed from ϕ_1 and Φ. A few of these possible vertices with legs attached are shown below.

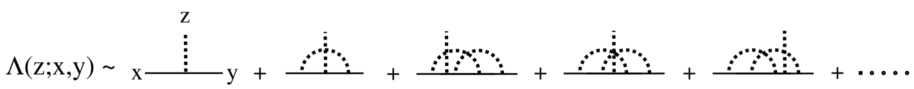

Figure 3. Diagrammatic expansion of Λ with legs attached.

[1] $\delta Z/\delta j_1(x) = \int \mathcal{D}(\phi_1,\phi_2,\Phi)\;\phi_1\, e^{-S}$

[2] Unless there is spontaneous symmetry breaking which gives a non-vanishing vacuum expectation value.

[3] $\langle\Phi\rangle = 1/Z\,\delta Z/\delta J$, therefore $\delta\langle\Phi\rangle/\delta J = \langle\Phi\Phi\rangle - \langle\Phi\rangle\langle\Phi\rangle$; however, if there is no spontaneous symmetry breaking the term with $\langle\Phi\rangle$ vanishes in the limit $J \to 0$

Substituting all of this into (2.11) gives

$$\left[-\partial_\mu\partial_\mu + m_1^2\right] G_1(x,y) \\ -g^2\int \mathrm{d}^4z\,\mathrm{d}^4z_1\,\mathrm{d}^4z_2\;\Delta_\Phi(x,z)G_1(x,z_1)\Lambda_1(z;z_1,z_2)G_1(z_2,y) = \delta^4(x-y). \quad (2.17)$$

This was the equation we were looking for. We write it in a more readable form:

$$\left[-\partial_\mu\partial_\mu + m_1^2\right] G_1(x,y) + \int \mathrm{d}^4z_2\;\Sigma_1(x,z_2)G_1(z_2,y) = \delta^4(x-y), \quad (2.18)$$

with

$$\Sigma_1(x,z_2) \equiv -g^2\int \mathrm{d}^4z\,\mathrm{d}^4z_1\;\Delta_\Phi(x,z)G_1(x,z_1)\Lambda_1(z;z_1,z_2), \quad (2.19)$$

or more symbolically

$$\left[\partial_\mu\partial_\mu - m_1^2 + \Sigma_1\right] G_1(x,y) = \delta^4(x-y). \quad (2.20)$$

If we ignore the self-energy terms (set $g = 0$) in (2.20), it reduces to the Klein-Gordon equation for the propagation of a free scalar particle – equation (A.11). Also using the integral definition of Σ we can arrive at a diagrammatic representation of the self-energy operator as shown in Figure 4.

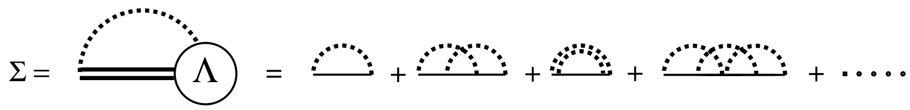

Figure 4. Diagrammatic representation of Σ.

2.2 Derivation of the Bethe-Salpeter Equation

In order to get information about a four-point function (propagation of two particles) we have to take a couple more derivatives with respect to the sources. We recall (2.6): $(x \to x_1)$

$$\left[\hat{M}\frac{\delta}{\delta j_1(x_1)} - j_1(x_1)\right] Z[j_1, j_2, J] = 0 \quad (2.21)$$

where

$$\hat{M} \equiv -\partial_\mu\partial_\mu + m_1^2 + g\frac{\delta}{\delta J(x)}. \quad (2.22)$$

Taking three functional derivatives with respect to j_1 and j_2 gives

$$\hat{M}\frac{\delta^4 Z}{\delta j_2(y_2)\delta j_1(y_1)\delta j_2(x_2)\delta j_1(x_1)} = \delta^4(x_1-y_1)\frac{\delta^2 Z}{j_2(y_2)j_2(x_2)}. \quad (2.23)$$

Writing this in terms of two and four-point functions gives:

$$\hat{M}G(x_1,y_1;x_2,y_2) = \delta^4(x_1-y_1)G_2(x_2,y_2). \quad (2.24)$$

Separate $\hat{M}$ into two terms:

$$\left[-\partial_\mu\partial_\mu + m_1^2 + \Sigma_1\right] G(x_1, y_1; x_2, y_2) = \delta^4(x_1 - y_1)G_2(x_2, y_2) + \left(-g\frac{\delta}{\delta J(x_1)} + \Sigma_1\right) G(x_1, y_1; x_2, y_2). \tag{2.25}$$

We can make use of (2.20) by multiplying by $G_1(z_1, x_1)$ and integrating over x_1 to give

$$G(x_1, y_1; x_2, y_2) = G_1(x_1, y_1)G_2(x_2, y_2) + \int \mathrm{d}^4 z_1 G_1(x_1, z_1) \left(-g\frac{\delta}{\delta J(z_1)} + \Sigma_1\right) G(z_1, y_1; x_2, y_2)\,. \tag{2.26}$$

Now we need to understand what the last term on the right hand side means. We expect that as in the case of the two-point function, this term is related to the two-particle self energy, i.e. the two-particle irreducible (2PI) graphs. Proving that this object does in fact generate the 2PI graphs is difficult, therefore, we will appeal to the diagrammatic technique used for the one-particle self energy. For example, consider the expansion of the four-point function

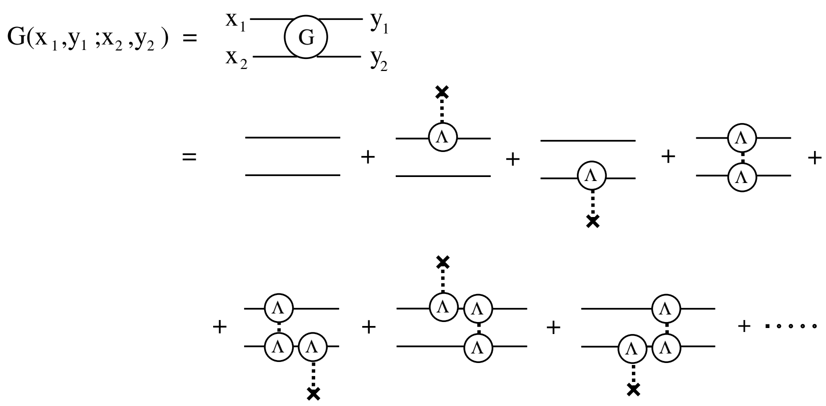

Figure 5. Expansion of the four-point function $G(x_1, y_1; x_2, y_2)$. All one-particle propagators are full propagators with $J = 0$.

Using the graphical technique for taking functional derivatives discussed earlier we generate the following

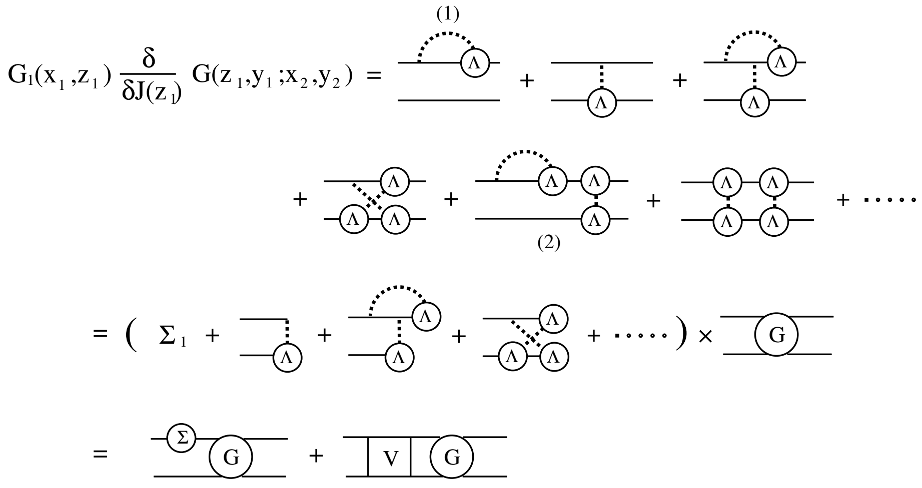

Figure 6. Functional derivative of $G(x_1, y_1; x_2, y_2)$ with respect to J. (1) and (2) indicate graphs that contribute to the self energy of particle one. The last two lines show the factorization of this into kernel, self energy, and $G(x_1, y_1; x_2, y_2)$.

This expansion also contains terms that contribute to the one-particle self energy indicated by the numbers (1) and (2) in Figure (6). These are eliminated by the subtraction of the one-particle self energy as seen in (2.26) leaving

$$
\begin{aligned}
G(x_1, y_1; x_2, y_2) &= G_1(x_1, y_1) G_2(x_2, y_2) + \\
&\int \mathrm{d}^4 z_1 \, \mathrm{d}^4 z_2 \, \mathrm{d}^4 z_1 \, \mathrm{d}^4 z_2 \; G_1(x_1, z_1) G_2(x_2, z_2) V(z_1, z_3; z_2, z_4) \, G(z_3, y_1; z_4, y_2). \quad (2.27)
\end{aligned}
$$

This is the Bethe-Salpeter equation. It can be written in an abbreviated form as

$$
G_{(12)} = G_1 G_2 + G_1 G_2 V G_{(12)}. \quad (2.28)
$$

In order to get this in terms of the connected scattering matrix with no legs we define $M \equiv (G_1 G_2)^{-1} G_c (G_1 G_2)^{-1}$ with $G_c \equiv G_{(12)} - G_1 G_2$. Doing this gives the equation

$$
M = V + V G_1 G_2 M \, . \quad (2.29)
$$

Since propagation and interactions are much easier to deal with in momentum space it is helpful to Fourier transform this equation. We can also use conservation of momentum to write this in terms of the relative and total momentum of the pair. Thus whenever we have a pair propagating, we can write $p_1 = \eta P + p$ and $p_2 = (1 - \eta) P - p$. Doing this gives

$$
M(p, q; P) = V(p, q; P) + \int \mathrm{d}^4 k \, V(p, k; P) G_1(\eta P + k, P) G_2((1-\eta) P - k, P) M(k, q, P). \quad (2.30)
$$

We can expand M in a Born series as

$$M = V + VG_1G_2V + VG_1G_2VG_1G_2V + \dots \tag{2.31}$$

which is just the scattering amplitude for ϕ_1, ϕ_2 scattering. However, it is possible that this series does not converge. In fact, the appearance of a bound state coincides with such a divergence, i.e. there is a pole in the scattering matrix [1]. We can separate the contribution from the bound state pole by expressing M as [5]

$$M(p, q; P) = \frac{\Gamma(p, P)\bar{\Gamma}(q, P)}{P^2 + M_B^2} + R(p, q; P), \tag{2.32}$$

where $R(p, q; P)$ has no pole at $P^2 = -M_B^2$ and Γ is the called the vertex function or Bethe-Salpeter wavefunction. Substituting this expression for M into (2.30) gives an equation for $\Gamma(p, P)$

$$\Gamma(p, P) = \int d^4k \, V(p, k; P) G_1(\eta P + k, P) G_2((1 - \eta)P - k, P) \Gamma(k, P) \, . \tag{2.33}$$

¿From this equation we see that the vertex function Γ tells us how to combine two off-shell propagating particles into a free propagating bound state, and likewise $\bar{\Gamma}$ tells us how to separate a bound state into two off-shell particles. All of these equations have accompanying diagrammatic representations as shown in Figure 7.

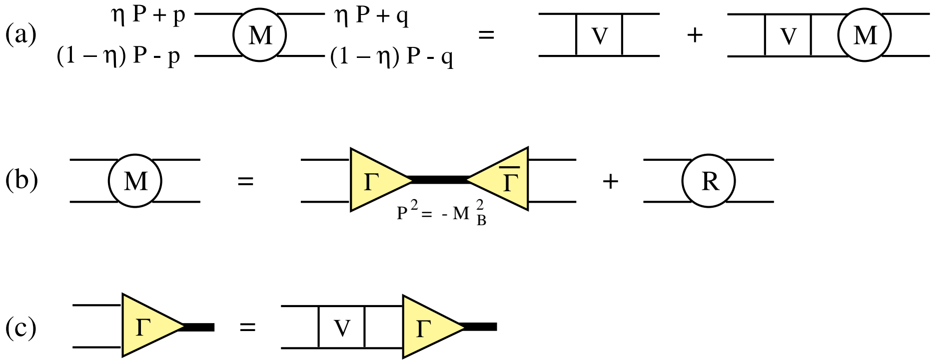

Figure 7. Diagrammatic representations of (a) (2.30) (b) (2.32) and (c) (2.33). All diagrams have legs attached.

2.3 The Ladder Approximation

In the previous section we obtained an integral equation for the Bethe-Salpeter vertex function $\Gamma(p, P)$ in terms of propagators and the 2PI kernel $V(p, k; P)$. Since the 2PI kernel is a sum of infinitely many terms we must truncate the sum after a finite number of diagrams. In fact we will retain only the simplest diagram in the expansion of the 2PI kernel, that of a single Φ exchange.[4] This is called the "ladder approximation". The ladder diagram may be

[4]This corresponds to taking the first diagram of Figure 6 line 3 and substituting the lowest order expression for Λ.

calculated from an effective action, which is obtained by performing one of three functional integrals exactly and approximating the remaining two.

We construct the generating functional for the Lagrangian density (2.3), with the path integral

$$Z[J,j_1,j_2] = \int \mathcal{D}(\Phi,\phi_1,\phi_2)\, e^{-S}\,, \tag{2.34}$$

where

$$\begin{aligned} S &= S_1 + S_2 + S_\Phi \\ S_i[\phi_i,j_i] &= \int \mathrm{d}^4x \left\{\frac{1}{2}\phi_i(x)(-\partial_\mu\partial_\mu + m_i^2)\phi_i(x) - j_i(x)\phi_i(x)\right\} \\ S_\Phi[\Phi,\phi_i;J] &= \int \mathrm{d}^4x \left\{\frac{1}{2}\Phi(x)(-\partial_\mu\partial_\mu + M^2)\Phi(x) + \frac{g}{2}\sum_{i=1}^{2}\phi_i^2(x)\Phi(x) - J(x)\Phi(x)\right\} \end{aligned} \tag{2.35}$$

Taking derivatives of $Z[J,j_i]$ with respect to the currents will generate all of the connected and disconnected Green's functions for the theory. Since S_Φ has the form of a Gaussian we may perform the functional integration over Φ exactly using standard techniques [8]. We obtain:

$$\begin{aligned} Z[J,j_1,j_2] &= \int \mathcal{D}(\phi_1,\phi_2)\, e^{-S'[\phi_i;J,j_i]} \\ S'[\phi_i;J,j_i] &= S_1 + S_2 + \frac{1}{2}\int \mathrm{d}^4x\, \ln\Delta_\Phi^{-1}(x,x) + \frac{1}{2}\int \mathrm{d}^4x \int \mathrm{d}^4y\, B(x)\Delta_\Phi(x,y)B(y) \end{aligned} \tag{2.36}$$

We have defined $\Delta_\Phi(x,y)$ so that

$$(-\partial_\mu\partial_\mu + M^2)\Delta_\Phi(x,y) = \delta^4(x-y)\,, \tag{2.37}$$

and

$$B(x) = J(x) - \frac{g}{2}\sum_{i=1}^{2}\phi_i^2(x)\,. \tag{2.38}$$

By performing the functional integral (2.35) exactly we have in effect fully quantized the Φ field. It is impossible to perform the two remaining functional integrals in (2.36) exactly and so the ϕ_1 and ϕ_2 fields must be approximated in some manner.

The simplest approximation we can perform is to simply evaluate the integrand at $\phi_1(x)$ and $\phi_2(x)$. This procedure is akin to totally neglecting the quantum nature of these two fields. When this is done the resulting "tree-level" generating functional describes two classical fields interacting with each other via a nonlocal potential $\Delta_\Phi(x-y)$.

$$Z_{\text{tree}}[J,j_i] = e^{-S_1 - S_2 + \frac{1}{2}\int \mathrm{d}^4x \int \mathrm{d}^4y\, B(x)\,\Delta_\Phi(x,y)\,B(y)} \tag{2.39}$$

The $\mathrm{Tr}(\ln(\Delta_\Phi^{-1}))$ term in (2.36) has been absorbed into the normalization constant $\mathcal{N}$.

The generator of *connected* Green's functions $W[J,j_i]$ is related to the functional $Z[J,j_i]$ by

$$Z[J,j_i] = e^{\,W[J,j_i]}\,, \tag{2.40}$$

and the effective action $\Gamma[\phi_i]$ is the partial Legendre transform of $W[J,j_i]$ [8],

$$\Gamma[J,\phi_i] = -W[J,j_i] + \sum_{i=1}^{2}\int \mathrm{d}^4x\, \phi_i(x)j_i(x)\,. \tag{2.41}$$

Comparison with the tree-level generating functional in (2.39) leads to the tree-level effective action,

$$\Gamma_{\mathrm{tree}}[J,\phi_i] = \frac{1}{2}\sum_{i=1}^{2}\int \mathrm{d}^4x\, \phi_i(x)\Big(-\partial_\mu\partial_\mu + m_i^2\Big)\phi_i(x) - \frac{1}{2}\int \mathrm{d}^4x \int \mathrm{d}^4y\, B(x)\Delta_\Phi(x,y)B(y)\,. \tag{2.42}$$

The ladder kernel is obtained by taking four derivatives of $\Gamma_{\mathrm{tree}}[J,\phi_i]$ with respect to the fields ϕ_1 and ϕ_2, and setting J to zero. In coordinate space we find

$$V_{\mathrm{ladder}}(x,x';y,y') = \left.\frac{\delta^4\Gamma_{\mathrm{tree}}[J,\phi_i]}{\delta\phi_2(y')\delta\phi_2(y)\delta\phi_1(x')\delta\phi_1(x)}\right|_{J=0} = -g^2\Delta_\Phi(x,y)\delta^4(x-x')\delta^4(y-y')\,. \tag{2.43}$$

3 Numerical Methods and Results

In this section we investigate an iterative method for solving the Bethe-Salpeter equation and present numerical results within the ladder approximation. The approach transforms the integral equation into a matrix equation which is then solved iteratively. This conversion is carried out on the Bethe-Salpeter equation (2.33) explicitly. Using this procedure we obtain vertex functions for the ground state as well as the first excited state. We go on to calculate the form factor and effective radius of the ground state. As a final note, we discuss a well-known peculiarity of the ladder approximation which is related to the fact that the center of momentum is ill defined for a relativistic problem. We show that this does not cause problems and affords stable solutions if the center of momentum parameter η is chosen reasonably.

To begin we show the steps used to convert $\Gamma(p,P)$ into a vector. The momentum dependence of the vertex function $\Gamma(p,P)$ is of the forms p^2, P^2, and $p\cdot P$. In Euclidean space we can use four dimensional spherical coordinates, and write

$$k_\mu = (k_x,k_y,k_z,k_t) \tag{3.1}$$

as

$$k_\mu = k(\cos\phi\sin\theta\sin\beta, \sin\phi\sin\theta\sin\beta, \cos\theta\sin\beta, \cos\beta)\,, \tag{3.2}$$

so that

$$\int \mathrm{d}^4k = \int_0^\infty k^3\mathrm{d}k \int_0^{2\pi}\mathrm{d}\phi \int_0^\pi \sin\theta\mathrm{d}\theta \int_0^\pi \sin^2\beta\mathrm{d}\beta\,. \tag{3.3}$$

ϕ and θ denote the usual three dimensional Euclidean spherical angles and β denotes the angle off the Euclidean time axis.

Choosing the total momentum P to be along the time axis, we expand $\Gamma(p,P)$ in terms of Tschebyshev polynomials[5]

$$\Gamma(p,P)=\sum_{a=0}^{\infty}\Gamma^a(p^2,P^2)\,T^a(\cos\beta)\,. \tag{3.4}$$

Substituting this into our Bethe-Salpeter equation (2.33), writing all variables in four dimensional spherical coordinates, multiplying both sides by $T^a(\cos\beta)$, integrating over β, and making use of the Tschebyshev's orthogonality properties, we obtain

$$\Gamma^a(p^2,P^2)=\sum_{b=0}^{\infty}\int_0^{\infty}\mathrm{d}q\mathcal{K}^{ab}(p^2,q^2;P^2)\Gamma^b(q^2,P^2), \tag{3.5}$$

where

$$\begin{aligned}\mathcal{K}^{ab}(p^2,q^2;P^2)=\frac{g^2}{\zeta\pi^4}q^3\int_0^{\pi}\mathrm{d}\beta'\sin^2\beta'\left(\int_0^{\pi}\mathrm{d}\beta\,T^a(\cos\beta)\Delta_\Phi(p-q)\right)\\ \times G_1(\eta P+q)G_2((1-\eta)P-q)T^b(\cos\beta')\end{aligned} \tag{3.6}$$

is the kernel and the Tschebyshev normalization gives $\zeta=2$ if $a=0$ and $\zeta=1$ otherwise, as described in Appendix C. The propagators are explicitly given by

$$\begin{aligned}\Delta_\Phi(p-q) &= \frac{1}{p^2+q^2-2pq\cos\beta'\cos\beta+m_\Phi^2}\\ G_1(\eta P+q) &= \frac{1}{-\eta^2M_B^2+q^2+2i\eta M_Bq\cos\beta'+m_1^2}\\ G_2((1-\eta)P-q) &= \frac{1}{-(1-\eta)^2M_B^2+q^2-2i(1-\eta)M_Bq\cos\beta'+m_2^2}.\end{aligned} \tag{3.7}$$

In writing (3.7) we have used the fact that $P^2=-M_B^2$, where M_B is the bound state mass. Examining (3.7) we see that there are no poles along the integration path as long as m_Φ is non-zero. This is the main advantage of working in Euclidean space. In our computations we use the small value of $m_\Phi\approx 0.01$ and observed that the computations were unaffected when m_Φ was varied.

It is a simple matter to convert the integral equation (3.5) into a matrix equation by a quantizing procedure involving Gaussian quadratures. The reader is directed to Appendix D for a brief introduction to Gaussian quadratures and the quantization of integral equations. We find

$$\lambda\Gamma_i^a=\sum_{bj}\mathcal{K}_{ij}^{ab}\Gamma_j^b\,, \tag{3.8}$$

where the Gaussian quadrature weights have been absorbed into $\mathcal{K}_{ij}^{ab}$ and λ has been inserted to make (3.8) more closely resemble an eigenvalue problem. The indices i and j correspond to the Gaussian mesh points and a and b denote Tschebyshev moments. We truncate the infinite sum of Tschebyshev moments and keep only the first five. Later we see that the zeroth Tschebyshev moment contributes to about 90% of the vertex function $\Gamma(p,P)$. The solution to the Bethe-Salpeter equation (2.33) corresponds to the eigenvector Γ_i^a that satisfies (3.8) with an eigenvalue of $\lambda=1$.

[5]The Tshebyshev polynomials $\{T^a(x)\}$ are a complete set of functions on the domain $[-1,1]$. Some details concerning the Tschebyshev polynomials are given in Appendix C.

3.1 The Method Of Iteration and The Democratic Method

Since we are only interested in solving the Bethe-Salpeter equation for the lowest energy bound state, and perhaps the first excited state, we can use the method of iteration. Consider the eigenvalue problem

$$\lambda Y_i = \sum_j A_{ij} Y_j. \tag{3.9}$$

Finding an eigenvalue λ which satisfies (3.9) is carried out by arbitrarily choosing a vector $\vec{Y}$ and multiplying it by $\mathbf{A}$ repeatedly until the (normalized) product approaches a limit. We show that if this iterative process does converge, it will generate the largest eigenvalue and its associated eigenvector.

Assume that (3.9) has N eigenvalues $\{\lambda_\alpha\}$ and for each eigenvalue λ_α there is a corresponding unit eigenvector $\vec{X}^\alpha$.[6] We order the eigenvalues in descending order, $\{\lambda_1, \lambda_2, \ldots, \lambda_N\}$ with $|\lambda_\alpha| \geq |\lambda_\beta|$ if $\alpha < \beta$. Let us assume that λ_1 is distinct from all other eigenvalues, but that the other eigenvalues can occur with any multiplicity whatsoever. This is the sole constraint placed on the eigenvalues. The assumption that λ_1 (the largest eigenvalue) is distinct implies that the ground state is not degenerate.

We arbitrarily choose a vector $\vec{Y}^{(0)}$ – the *zeroth iterate* – which is normalized in the same manner as the eigenvectors. We expand it in terms of the complete set of eigenvectors $\{\vec{X}^\alpha\}$ associated with $\mathbf{A}$.

$$\vec{Y}^{(0)} = \sum_{\alpha=1}^{N} c_\alpha \vec{X}^\alpha \tag{3.10}$$

Here the c_α are complex coefficients, and we will assume that $c_0 \neq 0$.[7] Upon substituting this into the matrix equation (3.9) we obtain the *first iterate*,

$$\vec{Y}^{(1)} \equiv \mathbf{A}\vec{Y}^{(0)} = \sum_{\alpha=1}^{N} \lambda_\alpha c_\alpha \vec{X}^\alpha. \tag{3.11}$$

Substitution of the first iterate into (3.9) leads to a result quadratic in λ_α. Repeating this procedure k times,

$$\vec{Y}^{(k)} \equiv \mathbf{A}^k \vec{Y}^{(0)} = \sum_{\alpha=1}^{N} (\lambda_\alpha)^k c_\alpha \vec{X}^\alpha. \tag{3.12}$$

Let us examine the ratio between ith components of two successive iterates $\vec{Y}^{(k)}$ and $\vec{Y}^{(k+1)}$.

$$\begin{aligned} \frac{Y_i^{(k+1)}}{Y_i^{(k)}} &= \frac{\sum_{\alpha=1}^{N} c_\alpha \lambda_\alpha^{k+1} X_i^\alpha}{\sum_{\alpha=1}^{N} c_\alpha \lambda_\alpha^{k} X_i^\alpha} \\ &= \lambda_1 \frac{1 + \sum_{\alpha=2}^{N} \frac{c_\alpha}{c_1}\frac{X_i^\alpha}{X_i^1}\left(\frac{\lambda_\alpha}{\lambda_1}\right)^{k+1}}{1 + \sum_{\alpha=2}^{N} \frac{c_\alpha}{c_1}\frac{X_i^\alpha}{X_i^1}\left(\frac{\lambda_\alpha}{\lambda_1}\right)^{k}} \end{aligned} \tag{3.13}$$

[6] The reader is warned not to confuse the "norm" of these vectors with the normalization of the Bethe-Salpeter vertex function $\Gamma(p, P)$! The "norm" used here is *any* operation that satisfies the three properties required for a norm of a vector space [10].

[7] We explicitly assume that $\vec{Y}^{(0)}$ is *not* orthogonal to $\vec{X}^1$, for ease of discussion. If c_0 was identically zero, after the first iteration, round-off errors would prevent c_0 from remaining zero, and the method then proceeds as discussed.

For large k the ratio approaches λ_1 since we have assumed that $|\lambda_1|$ is (strictly) greater than $|\lambda_\alpha|$, for $\alpha > 1$.

$$\frac{Y_i^{(k+1)}}{Y_i^{(k)}} = \lambda_1 - \mathrm{O}\left(\frac{\lambda_2}{\lambda_1}\right)^k \tag{3.14}$$

For the types of kernels we will consider, this process converges to several decimal places in very few iterations. Rapid convergence is the main benefit of the method of iteration. On the other hand, it is possible that many iterations may be required for a system in which $|\lambda_2|$ is approximately equal to $|\lambda_1|$.

We have not only succeeded in computing the largest eigenvalue with relative ease, but we have also computed the associated eigenvector. When k is large enough to satisfy (3.14), the ratio between any component of the kth and $k+1$th iterates will be very nearly λ_1. Therefore

$$\lambda_1 \vec{Y}^{(k)} \approx \vec{Y}^{(k+1)} = \mathbf{A}\vec{Y}^{(k)}\,, \tag{3.15}$$

which is the definition of the eigenvector $\vec{X}^1$! We find that after a sufficient number of iterations $\vec{Y}^{(k)} \approx \vec{X}^1$.

We have found in our model that usually only 10–15 iterations are required for accurate determination of λ_1. The method of iteration requires only a small number matrix multiplications and is therefore much faster and more accurate than performing a matrix inversion or diagonalization which requires many more multiplication operations as well as division and subtraction operations (that are inherently less accurate than multiplication). However, the reader is reminded that we have so far only obtained the largest eigenvalue/vector, whereas other methods allow one to obtain all of the eigenvalues/vectors. We show below that the method of iteration can be used to obtain other eigenvalues/vectors as well. This can be done with little work and minimal computational cost; the price we pay is some loss of accuracy. To obtain the second largest eigenvalue we examine the ratio

$$\lambda_2(i) \approx \frac{Y_i^{(m+1)} - \lambda_1 Y_i^{(m)}}{Y_i^{(m)} - \lambda_1 Y_i^{(m-1)}}. \tag{3.16}$$

In general the calculated value for λ_2 will depend on which *component* i is used. To extract a sensible λ_2 we would like to have $m \ll k$ because when $m \approx k$ the iterates $\vec{Y}^m$ will be dominated by $\vec{X}_1$. This dominance will cause inaccuracy in the subtraction indicated in (3.16). The same aspect of the iteration method that gives such rapid convergence to λ_1 destroys information about $\lambda_2, \lambda_3, \ldots$.

In order to deal with this complication, we calculate and store the first $k+1$ iterates, where k is large enough for sufficient convergence of λ_1. We then recall the earlier iterates and subtract off the contribution due to $\vec{X}^1$, as in (3.16). However, for each iterate we will obtain a different value of λ_2 from (3.16) and the question will then be: Which value is closest to the true λ_2?

To decide which is the best value for λ_2, we compute the standard deviation of $\lambda_2(i)$ at each intermediate iteration m. The set with the smallest standard deviation is kept and the mean recorded. We call this the *democratic method*, because it involves getting the "opinion" of each of the N components of the mth iterate $\vec{Y}^{(m)}$.

The validity of the democratic method may be clarified by observing the evolution of the iterates through the vector space spanned by $\{\vec{X}^\alpha\}$. Assume $\vec{Y}^{(0)}$ is linearly dependent on all of the eigenvectors vectors $\vec{X}^\alpha$ as shown in (3.10). As the iteration process continues, the iterates begin to converge to $\vec{X}^1$, until finally, the kth iterate $\vec{Y}^{(k)}$ contains virtually none of the other eigenvectors. The effect of the iterations is to dampen out $\vec{Y}^{(0)}$'s dependence on all of the eigenvectors except $\vec{X}^1$. At some intermediate iteration, say mth, it may happen that all eigenvectors have been washed away except for the first two, so that

$$\vec{Y}^{(m)} = \tilde{c}_1\vec{X}^1 + \tilde{c}_2\vec{X}^2 + \mathrm{O}\left(\frac{\lambda_3}{\lambda_2}\right). \tag{3.17}$$

Since we have already obtained $\vec{X}^1$ to any degree of accuracy, we can easily extract $\vec{X}^2$ from (3.17). The question that remains is to determine the best value of m to do this. m must be large enough so that $\frac{\lambda_3}{\lambda_2}$ is small, but small enough that $\frac{\lambda_2}{\lambda_1}$ is *not* small. The appropriate iteration m is chosen by the democratic method. The reader is directed to Appendix E for a discussion of the democratic method.

3.2 Eigenvalues and Vertex Functions

We search for a bound state comprised of two distinguishable particles of mass $m_1 = m_2 = 20.0$, which interact via the exchange of a massless scalar boson with coupling constant of $\frac{g}{m_1} = 17.32$. These values have been chosen for convenience.

To find the ground state mass and vertex function, we begin with an arbitrary zeroth iterate $\vec{\Gamma}^{(0)}$ and a small value of the total momentum P. After twenty iterations we extract the largest eigenvalue λ_1. The value of λ_1 is recorded, another slightly larger momentum P is chosen, and the process is repeated until the breakup threshold $P^2_{\text{Threshold}} = -(m_1 + m_2)^2$ is reached. We have solved the Bethe-Salpeter equation if we can find a value of the total momentum P ($|P^2| < |P^2_{\text{Threshold}}|$) where $\lambda_1 = 1$. Over a broad range of total momentum P, we compute the values of λ_1 shown in Figure 8 as the solid curve. The bound state mass is found by reading off the energy for which $\lambda_1 = 1$. We find that the ground state has a mass of $M_B^{(1)} = 23.97$.

Table 1 shows the value of λ_1 after each successive iteration along with an estimation of the error. For brevity only the even numbered iterations have been shown. From Table 1 we see that even for a physically reasonable problem, the rate of convergence of this method is very rapid.

Convergence for Bethe-Salpeter Kernel		
(i)	λ_1 after ith iteration	$\left(\frac{\lambda_i-\lambda_{i-1}}{\lambda_i+\lambda_{i-1}}\right)$
2	1.38407747874241682	0.5941×10^{-0}
4	1.03774749530195076	-0.7687×10^{-1}
6	1.00657336755871496	-0.7103×10^{-2}
8	1.00385518307496047	-0.6124×10^{-3}
10	1.00362391917986571	-0.5193×10^{-4}
12	1.00360435068994769	-0.4392×10^{-5}
14	1.00360269647441003	-0.3712×10^{-6}
16	1.00360255665753129	-0.3137×10^{-7}
18	1.00360254484027878	-0.2652×10^{-8}
20	1.00360254384149328	-0.2241×10^{-9}

Table 1. Convergence of iteration method using the Bethe-Salpeter kernel. Eigenvalue and the fractional change after the ith iteration are shown.

With an accurate value for λ_1, we compute the next eigenvalue using the democratic method. The resulting values for λ_2 are indicated by the dashed curve in Figure 8. By reading off the value for the total momentum when $\lambda_2 = 1$ we observe the mass of the first excited state to be $M_B^{(2)} = 37.58$.

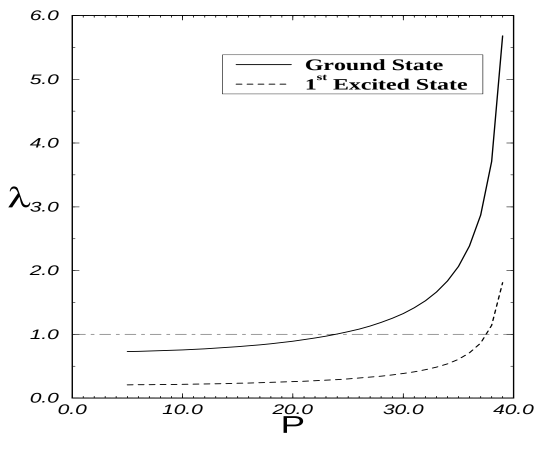

Figure 8. Eigenvalues λ vs total CM energy $|P|$. Bound state occurs at $|P| = M_B$ when $\lambda = 1$.

Once we have extracted these eigenvalues and eigenvectors, we have the means to obtain all of the information about the bound states. The eigenvectors are the vertex functions of the bound states. As such, they relate the properties of the bound state to the constituents. We calculate the momentum dependence of the interaction between the bound state and an external Φ field – the *form factor*.

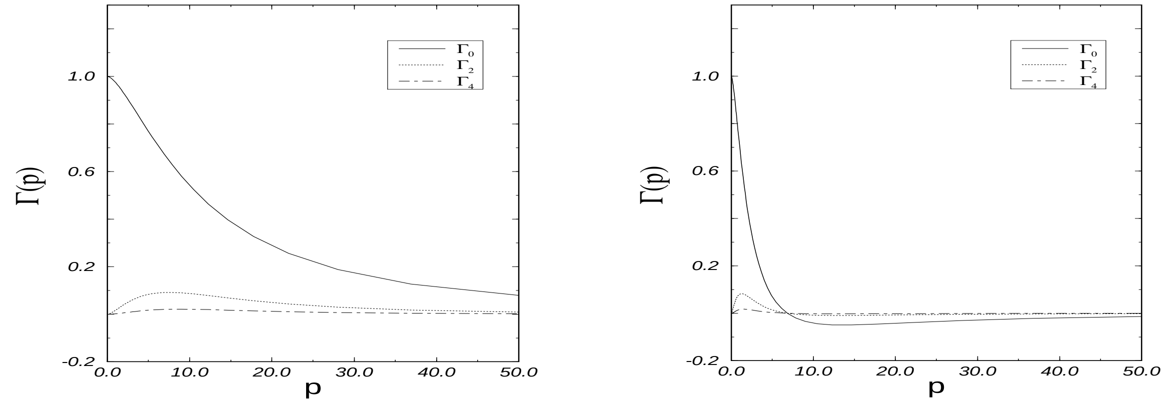

Figure 9. Vertex function for (a) Ground State (b) 1^{st} Excited State.

Before calculating the form factor we exhibit the vertex functions for the two bound states. The scales on each are arbitrarily chosen so that the maximum is 1.[8] Figures 9a and 9b clearly exhibit the dominance of the zeroth Tschebyshev moment, as mentioned earlier. The second moment contributes less than 10%, and the fourth moment is totally negligible.

Furthermore, only the even Tschebyshev moments contribute to the vertex function $\Gamma(p, P)$ due to a symmetry of the kernel. If one simultaneously performs the change of variables $\beta' \rightarrow \beta' - \pi$ and $p \rightarrow -p$ in (3.6), we observe a phase change of $(-1)^b$. Thus for odd Tschebyshev moments the kernel vanishes.

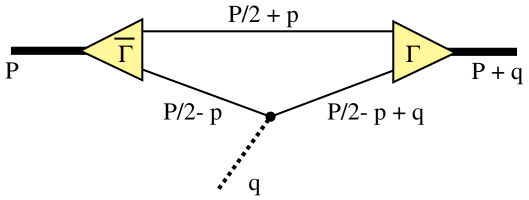

Figure 10. Ladder contribution to form factor.

Next we compute the scalar form factor (in the space-like region) and scalar charge radius of our bound state. Consider the Feynman diagram of Figure 10 which depicts the coupling of a Φ field to one of the constituents. The integral expression for the form factor is

$$F(q^2) \;\propto\; \frac{g}{2}\int \frac{\mathrm{d}^4k}{(2\pi)^4}\, \bar{\Gamma}(k, P+q)\, G_1(P/2+k) \times G_2(P/2-k)\, G_2(P/2-k+q)\, \Gamma(k,P) + (1 \leftrightarrow 2)\,. \quad (3.18)$$

[8]Normally, the Bethe-Salpeter vertex function must be normalized in a very specific manner but we have not done this. To obtain the form factors it is unnecessary.

We perform the integrations in the Breit frame:

$$\begin{aligned} q_\mu &= (0,0,q,0) \\ P_\mu &= (0,0,\frac{-1}{2}q, i\sqrt{M_B^2+\frac{q^2}{4}}) \\ k_\mu &= k(\cos\phi\sin\theta\sin\beta, \sin\phi\sin\theta\sin\beta, \cos\theta\sin\beta, \cos\beta) \end{aligned} \tag{3.19}$$

It is reasonable to maintain only the zeroth order Tshebyshev moment when performing the integral. Figure 9a clearly shows that this moment gives the dominant contribution to the vertex function.

The resulting form factor for the ground state is displayed in Figure 11. The plot shows the form factor over a large space-like region. From the slope of the form factor at $q^2 = 0$, we obtain the scalar radius of our ground state.

$$\langle r^2\rangle^{\frac{1}{2}} = \left(-6\frac{\mathrm{d}}{\mathrm{dq}^2}\ln F(q^2)\right)^{\frac{1}{2}}_{q^2=0} = 0.409 \tag{3.20}$$

The radius is given in inverse mass units.

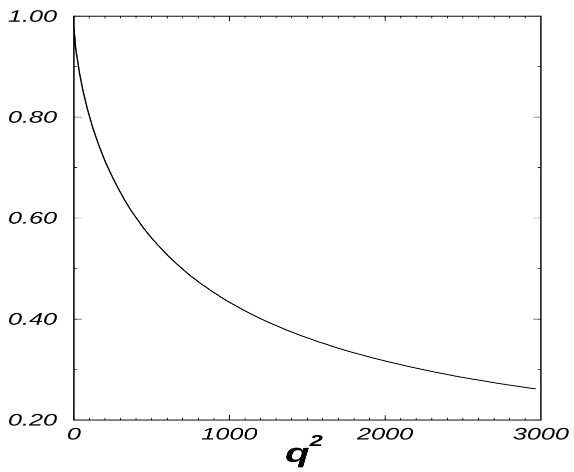

Figure 11. Form factor $F(q^2)$ of ground state.

3.3 η Dependence of the Ladder Approximation

To obtain solutions of the Bethe-Salpeter equation we have worked in the ladder approximation, in which the complete 2PI kernel is replaced by a single diagram. The ladder diagram has a very unique feature which separates it from all others in the kernel. It is the only diagram which has a particle exchange that is explicitly independent of the total momentum P. This fact is related to some well-known peculiarities; most notably, the ladder approximation's inability to correctly describe the static limit. That is, when one of the constituents becomes infinitely massive, the Bethe-Salpeter equation in the ladder approximation does *not* reduce to the Klein-Gordon equation [11]. Secondly, solutions of the Bethe-Salpeter equation in the ladder approximation exhibit a dependence on the CM parameter η which determines how the total momentum is shared amongst the two constituents:

$$\begin{aligned} p_1 &= \eta P + p \\ p_2 &= (1-\eta)P - p \end{aligned} \tag{3.21}$$

where p_1 and p_2 are the four momenta of particles 1 and 2, respectively. Here, η takes on *any* arbitrary value between 0 and 1, in contrast to the non-relativistic case where η is determined. The difference arises with the non-relativistic identification that

$$\vec{p} = m\dot{\vec{x}}. \tag{3.22}$$

This constrains η to take on the particular value

$$\eta = \frac{m_1}{m_1 + m_2}\,. \tag{3.23}$$

We do not expect that the solution to the full Bethe-Salpeter equation has a dependence on η, but unfortunately, the ladder approximation does. Throughout this paper we have used $\eta = \frac{1}{2}$.

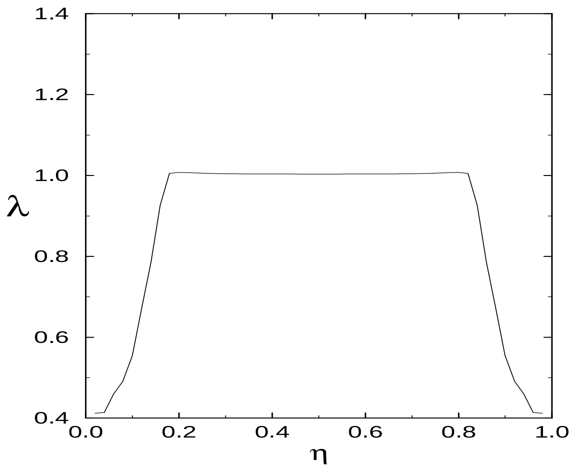

Figure 12. η dependence of the largest eigenvalue in the ladder approximation.

In Figure 12 we see how the eigenvalue λ_1 computed at the ground state energy, varies with η. For η between 0.2 and 0.8 there is virtually no effect on the observed eigenvalues. At $\eta = \frac{1}{2}$, there is a local minimum. For this value, the solution is affected by small perturbations of η the least. We are pleased to see that this minimum coincides with the value that seems to be the most natural choice for a system in which $m_1 = m_2$. A similar characteristic[9] was found to be present in the more complicated calculations of antiquark–quark bound states of Munczek and Jain [12].

It is interesting to note that the local minimum in Figure 12 evolves in a natural way as m_1 increases and m_2 decreases (keeping $m_1 + m_2$ fixed). The case when $m_1 = 26.66$ and $m_2 = 13.33$ (resulting in a $M_B^{(1)} = 23.2$) is shown in Figure 13. The local minimum has now moved to $\eta = 0.805$. With this observation, it is reasonable to compute solutions at this stable value of η. In this manner, the ladder approximation seems to afford consistent solutions.

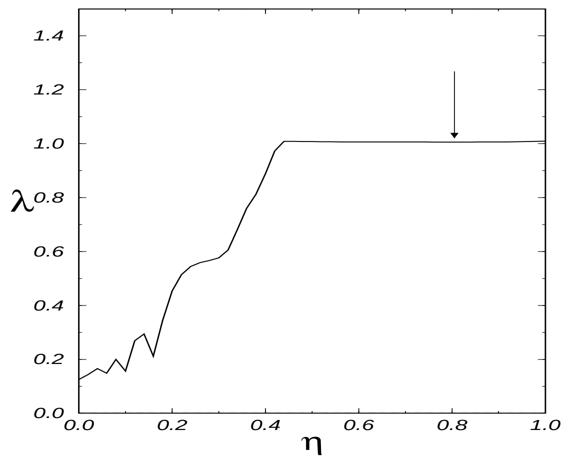

Figure 13. η dependence of largest eigenvalue when $m_1 = 26.66$ and $m_2 = 13.33$. The observed local minimum at $\eta = 0.805$ is indicated. Values of λ with $\eta < 0.2$ did not converge well.

4 Conclusion

We have shown that working in Euclidean space allows numerical solution of the Bethe-Salpeter equation without three-dimensional reduction. Using this method we eliminate the ambiguities associated with different reductions, allowing more concrete statements to be made about relativistic bound states. With this method we obtain the bound state wavefuctions as well as masses. Knowledge of these enables us to make predictions of the bound state spectrum and measurables such as the form factor. Future work will address the renormalization of the B-S equation. Specifically, by introducing infrared and ultraviolet cutoffs into the theory we can study the transition from free particles to bound states using a renormalization group flow equation. We have also outlined the derivation of the B-S

[9] "Similar characteristic" in the sense that Munczek and Jain report this critical point to be a *maximum*. The discrepancy between their works and this one is not understood by the current authors. However, we have found that systems with $m_1 > 10\ m_2$ have a minimum that becomes so shallow it is indistinguishable from the surrounding plateau, and so could *resemble* a local maximum.

equation and pointed out its connection to other field equations such as the Schwinger-Dyson equation. The goals of this paper were pedagogical but we hope to have laid the groundwork for more detailed investigations of the structure of bound states within QED and QCD.

5 Acknowledgements

The authors wish to express their thanks to Prof. W. W. Buck for sharing his insight and experience with us early in our investigations. One of us (MP) is also grateful to Dr. C. D. Roberts for first bringing the iterative method to our attention and continually providing us with many invaluable insights. One of us (MK) would like to thank Dr. John Dawson for his assistance, and for always being a good listener. The authors would also like to thank the Shaman Stick Brotherhood. This work was supported in part by the Division of Educational Programs, Argonne National Laboratory, under contract W-31-109-ENG-38.

A Going from Minkowski to Euclidean Space

In this appendix we will show how to tranform a free scalar Lagrangian and generating functional from Minkowski space to Euclidean space and derive the free propagator in Euclidean space. The generating functional for a free scalar field in Minkowski space (metric $g_{\mu\nu} = (1, -1, -1, -1)$) is given by

$$Z \equiv \int \mathcal{D}(\phi)\ e^{iS}, \tag{A.1}$$

where the action S is given by

$$S = \int \mathrm{d}^4x \left(\mathcal{L} + j\phi\right), \tag{A.2}$$

with

$$\mathcal{L} = \frac{1}{2}\left[\partial_\mu\phi\partial^\mu\phi - m^2\phi^2\right] \ . \tag{A.3}$$

To transform this to Euclidean space we make the substitutions

$$x_4 = ix_0 \qquad x_\mu x^\mu = -x^E_\mu x^E_\mu = -\sum_{i=1}^{4} x_i^2 \tag{A.4}$$

and

$$\partial_4 = -i\partial_0 \qquad \partial_\mu\phi\partial^\mu\phi = -\partial^E_\mu\phi\partial^E_\mu\phi = -\sum_{i=1}^{4}(\partial_i\phi)^2. \tag{A.5}$$

Thus, we have

$$Z = e^{i\left[-i\int \mathrm{d}^4x_E\,(-\mathcal{L}_E + j\phi)\right]} \equiv e^{-S_E}, \tag{A.6}$$

where

$$\mathcal{L}_E = \frac{1}{2}\left(\partial^E_\mu\phi\partial^E_\mu\phi + m^2\phi^2\right) \ , \tag{A.7}$$

and

$$S_E = \int \mathrm{d}^4 x_E \, \{\mathcal{L}_E - j\phi\}, \tag{A.8}$$

where the subscript E indicates the Euclidean space version. We do not use these subscripts for the body of the paper since everything we do is in Euclidean space. The integral over x_4 now has the limits $-i\infty \to i\infty$. In order to transform this to an integration along the real x_4 axis we can make use of the analyticity of n-point functions and the Cauchy theorem to rotate the contour back to the real axis [8]. To obtain the equations of motion in Euclidean space we can use the Euler-Lagrange equations

$$\frac{\delta S_E}{\delta\phi(x)} = \frac{\partial\mathcal{L}}{\partial\phi} - \partial_\mu \frac{\partial\mathcal{L}}{\partial(\partial_\mu\phi)} - j = 0, \tag{A.9}$$

where j is a generalized force or source. Applying this to the free Euclidean Lagrangian gives

$$(-\partial_\mu\partial_\mu + m^2)\phi = j. \tag{A.10}$$

The Green's function or two-point function is defined as the impulse response of a system

$$(-\partial_\mu\partial_\mu + m^2)G(x,y) = \delta^4(x-y). \tag{A.11}$$

We can derive the momentum space representation of G by writing the delta function as a sum over all Fourier modes and expressing $G(x,y)$ in terms of its Fourier transform (assuming translational invariance in time and space). Writing

$$G(x,y) = \int \frac{\mathrm{d}^4 p}{(2\pi)^4} G(p)\, e^{-ip_\mu(x-y)_\mu}\,, \tag{A.12}$$

we find

$$G(p) = (p^2 + m^2)^{-1}\,. \tag{A.13}$$

Note that the poles in the denominator are now located at $p_4 = \pm i E_p$, where $E_p = \sqrt{p^2 + m^2}$.

B Alternative Derivation of the Bethe-Salpeter Equation

Following a suggestion of Fred Cooper [13], we present here an alternative derivation of the Bethe-Salpeter equation, introducing an auxiliary field to represent the bound state [14]. We begin with the generating functional,

$$Z[j_i] = \int \mathcal{D}(\phi_1, \phi_2, \Phi) e^{-S[\phi_i, \Phi; j_i]}\,, \tag{B.1}$$

where

$$\begin{aligned} S &= S_1 + S_2 + S_\Phi \\ S_i[\phi_i, j_i] &= \int \mathrm{d}^4 x \left\{ \frac{1}{2}\phi_i(x)(-\partial_\mu\partial_\mu + m_i^2)\phi_i(x) - j_i(x)\phi_i(x) \right\} \\ S_\Phi[\Phi, \phi_i; J] &= \int \mathrm{d}^4 x \left\{ \frac{1}{2}\Phi(x)(-\partial_\mu\partial_\mu + M^2)\Phi(x) + g\sum_{i=1}^{2} \phi_i^2(x)\Phi(x) \right\}. \end{aligned} \tag{B.2}$$

We have not introduced a source for the Φ field, because we are not interested in its propagator. We can perform the functional integral over this field exactly, since it has a Gaussian form:

$$
\begin{aligned}
Z[j_i] &= \int \mathcal{D}(\phi_1, \phi_2)\, e^{-S'[\phi_i;j_i]} \\
S'[\phi_i; J, j_i] &= S_1 + S_2 + \frac{1}{2}\int \mathrm{d}^4x \,\ln \Delta_\Phi^{-1}(x,x) \\
&+ \frac{g^2}{2}\int \mathrm{d}^4x \int \mathrm{d}^4y \,\sum_{i=1}^{2} \phi_i^2(x)\Delta_\Phi(x,y)\sum_{j=1}^{2}\phi_j^2(y)\,,
\end{aligned}
\tag{B.3}
$$

where we have defined $\Delta_\Phi(x,y)$ so that

$$
(-\partial_\mu\partial_\mu + M^2)\Delta_\Phi(x,y) = \delta^4(x-y)\,. \tag{B.4}
$$

We will absorb the ln term into the normalization of the generating functional, since it is a constant and does not contribute to the overall dynamics.

Now, we can introduce an auxiliary field $B(x,y)$ into the generating functional by multiplying Z by a constant:

$$
\begin{aligned}
\text{constant} &= \int \mathcal{D}(B)\exp\Big\{\int \mathrm{d}^4x \int \mathrm{d}^4y \,\{-\frac{1}{2}[\phi_i(x)\phi_j(y) - B_{ij}(x,y)] \\
&\times \; G_{ijkl}(x,y)[\phi_k(x)\phi_l(y) - B_{kl}(x,y)]\} - J_{ij}(x,y)B_{ij}(x,y)\Big\}\,.
\end{aligned}
\tag{B.5}
$$

Here, $B(x,y)$ represents a composite field for the bound state, J is a source term for this field, and G is a constant. Notice that if we choose

$$
G_{ijkl}(x,y) = g^2\delta_{ik}\delta_{jl}\Delta_\Phi(x,y)\,, \tag{B.6}
$$

we can exactly cancel the quartic term in the generating functional, giving

$$
\begin{aligned}
Z[j_i, J_{ij}] &= \int \mathcal{D}(\phi_1, \phi_2, B) e^{-S''[\phi_i, B_{ij}; j_i, J_{ij}]} \\
S'' &= \sum_i S_i + \int \mathrm{d}^4x \int \mathrm{d}^4y \,\Big\{g^2\phi_i(x)\phi_j(y)B_{ij}(x,y)\Delta_\Phi(x,y) \\
&- \frac{g^2}{2}B_{ij}(x,y)B_{ij}(x,y)\Delta_\Phi(x,y) - J_{ij}(x,y)B_{ij}(x,y)\Big\}\,.
\end{aligned}
\tag{B.7}
$$

Writing S_i as

$$
S_i = \int \mathrm{d}^4x \int \mathrm{d}^4y \,\Big\{\frac{1}{2}\phi_i(x)g_{ij}^{-1}(x,y)\phi_j(y)\Big\} - \int \mathrm{d}^4x \, j_i(x)\phi_i(x)\,, \tag{B.8}
$$

where g_{ij} satisfies

$$
(-\partial_\mu\partial_\mu + m_i^2)g_{ij}(x,y) = \delta_{ij}\delta^4(x-y)\,, \tag{B.9}
$$

enables us to perform the ϕ_i integrals, since they are now in a quadratic form. The result is:

$$
\begin{aligned}
Z[j_i, J_{ij}] &= \int \mathcal{D}(B) e^{-S'''[B_{ij}; j_i, J_{ij}]} \\
S'''[B_{ij}] &= \int \mathrm{d}^4x \int \mathrm{d}^4y \,\Big\{-\frac{1}{2}j_i(x)G_{ij}(x,y)j_j(y) + \frac{1}{2}\mathrm{Tr}\ln\{G_{ij}^{-1}(x,y)\} \\
&- \frac{g^2}{2}B_{ij}(x,y)B_{ij}(x,y)\Delta_\Phi(x,y) - J_{ij}(x,y)B_{ij}(x,y)\Big\}\,,
\end{aligned}
\tag{B.10}
$$

where

$$G^{-1}_{ij}(x,y) = g^{-1}_{ij}(x,y) + 2g^2 B_{ij}(x,y)\Delta_\Phi(x,y)\,. \tag{B.11}$$

We are now able to perform the B integral using the method of steepest descent, expanding the action S''' about its stationary point. The necessary derivatives can be performed using the following:

$$\begin{aligned}
\frac{\delta G^{-1}_{\alpha\beta}(a,b)}{\delta B_{ij}(x,y)} &= 2g^2\Delta_\Phi(x,y) \\
\frac{\delta G_{kl}(w,z)}{\delta B_{ij}(x,y)} &= -2g^2 G_{ki}(w,x)\Delta_\Phi(x,y)G_{jl}(y,z)\,.
\end{aligned} \tag{B.12}$$

The first step is to perform two functional derivatives of the action, S''', with respect to the auxiliary field B. The first derivative gives:

$$\begin{aligned}
\frac{\delta S'''[B]}{\delta B_{ij}(x,y)} &= g^2\varphi_i(x)\Delta_\Phi(x,y)\varphi_j(y) + g^2 G_{ij}(x,y)\Delta_\Phi(x,y) \\
&- g^2 B_{ij}(x,y)\Delta_\Phi(x,y) - J_{ij}(x,y)\,,
\end{aligned} \tag{B.13}$$

where we have defined

$$\varphi_i(x) = \int \mathrm{d}^4y\, G_{ij}(x,y)j_j(y)\,. \tag{B.14}$$

At the stationary point, the first derivative of S''' with respect to B is zero. Performing one more derivative gives:

$$\begin{aligned}
-H^{-1}_{lm;ij}(w,z;x,y) &\equiv \frac{\delta^2 S}{\delta B_{lm}(w,z)\delta B_{ij}(x,y)} \\
&= 2g^4[G_{il}(x,w)\Delta_\Phi(w,z)\varphi_m(z)\Delta_\Phi(x,y)\varphi_j(y) \\
&+ \varphi_i(x)G_{jl}(y,w)\Delta_\Phi(x,y)\Delta_\Phi(w,z)\varphi_m(z)] \\
&- 2g^4 G_{il}(x,w)\Delta_\Phi(w,z)G_{mj}(z,y)\Delta_\Phi(x,y) \\
&- g^2\Delta_\Phi(x,y)\delta^4(x-w)\delta^4(y-z)\delta_{il}\delta_{jm}\,.
\end{aligned} \tag{B.15}$$

When the sources are set equal to zero, (B.13) gives, at the stationary point,

$$G_{ij}(x,y) = B_{ij}(x,y)\,, \tag{B.16}$$

and (B.15) gives:

$$\begin{aligned}
H^{-1}_{lm;ij}(w,z;x,y) &= 2g^4 G_{il}(x,w)\Delta_\Phi(w,z)G_{mj}(z,y)\Delta_\Phi(x,y) \\
&+ g^2\Delta_\Phi(x,y)\delta^4(x-w)\delta^4(y-z)\delta_{il}\delta_{jm}\,.
\end{aligned} \tag{B.17}$$

We can now do the functional integral over B:

$$\begin{aligned}
Z[j_i, J_{ij}] &= \int \mathcal{D}(B)e^{-S'''[B]} \equiv e^W \\
W[j_i, J_{ij}] &= -S[B^0] - \frac{1}{2}\mathrm{Tr}\ln H\,.
\end{aligned} \tag{B.18}$$

We are now in a position to derive the Bethe-Salpeter equation, in terms of two-point and four-point Green's functions, by taking derivatives of W with respect to the sources. Since J_{ij} is a composite current, we need to calculate

$$G_{ij;kl}(x,y;w,z) = \frac{\delta^3 W}{\delta j_i(x)\,\delta j_j(y)\,\delta J_{kl}(w,z)}\,. \tag{B.19}$$

Note that this is a mixed functional derivative.

The functional derivative with respect to J_{ij} can be performed by noting

$$B_{ij}(x,y) = \frac{1}{Z}\frac{\delta Z}{\delta J_{ij}(x,y)} = \frac{\delta W}{\delta J_{ij}(x,y)}\,. \tag{B.20}$$

We will only perform the calculation to first order for now, by neglecting the terms in H. This can be done by taking an implicit derivative of (B.13), with respect to $j_j(y)$:

$$\begin{aligned}
& g^2\Delta_\Phi(w,z)G_{lj}(w,y)\varphi_m(z) \\
- \;& 2g^4\int \mathrm{d}^4p\int \mathrm{d}^4a\int \mathrm{d}^4b\, G_{l\alpha}(w,a)\left[\frac{\delta B_{\alpha\beta}(a,b)}{\delta j_j(y)}\Delta_\Phi(a,b)\right] G_{\beta m}(b,p)\Delta_\Phi(w,z)\varphi_m(z) \\
+ \;& g^2\varphi_l(w)\Delta_\Phi(w,z)G_{mj}(z,y) \\
- \;& 2g^4\int \mathrm{d}^4p\int \mathrm{d}^4a\int \mathrm{d}^4b\,\varphi_l(w)\Delta_\Phi(w,z)G_{m\alpha}(z,a)\left[\frac{\delta B_{\alpha\beta}(a,b)}{\delta j_j(y)}\Delta_\Phi(a,b)\right] G_{\beta l}(b,p) \\
- \;& 2g^4\int \mathrm{d}^4a\int \mathrm{d}^4b\, G_{l\alpha}(w,a)\frac{\delta B_{\alpha\beta}(a,b)}{\delta j_j(y)}\Delta_\Phi(a,b)G_{\beta m}(b,z)\Delta_\Phi(w,z) \\
- \;& g^2\frac{\delta B_{lm}(w,z)}{\delta j_j(y)}\Delta_\Phi(w,z) = 0\,.
\end{aligned} \tag{B.21}$$

Note that when the sources are set equal to zero, we get

$$-g^2\Delta_\Phi(w,z)\left\{\frac{\delta B_{lm}(w,z)}{\delta j_j(y)} + 2g^4\int \mathrm{d}^4a\int \mathrm{d}^4b\,\frac{\delta B_{\alpha\beta}(a,b)}{\delta j_j(y)}\Delta_\Phi(a,b)G_{\beta m}(b,z)\right\} = 0\,, \tag{B.22}$$

or

$$\int \mathrm{d}^4a\int \mathrm{d}^4b\, H^{-1}_{lm;\alpha\beta}(w,z;a,b)\frac{\delta B_{\alpha\beta}(a,b)}{\delta j_j(y)} = 0\,, \tag{B.23}$$

which proves that

$$\frac{\delta B_{\alpha\beta}(a,b)}{\delta j_j(y)} = 0\,, \tag{B.24}$$

since we know that H^{-1} is *not* zero. Now we just have to take one more derivative of (B.21). Since we will be setting the sources equal to zero at the end, we only need to consider terms which will survive. The final result is:

$$\begin{aligned}
& [G_{lj}(w,y)G_{mi}(z,x) + G_{li}(w,x)G_{mj}(z,y)]\Delta_\Phi(w,z) \\
- \;& 2g^2\int \mathrm{d}^4a\int \mathrm{d}^4b\, G_{l\alpha}(w,a)\frac{\delta^2 B_{\alpha\beta}(a,b)}{\delta j_i(x)\delta j_j(y)}G_{\beta m}(b,z)\Delta_\Phi(w,z) \\
- \;& \frac{\delta^2 B_{lm}(w,z)}{\delta j_i(x)\delta j_j(y)}\Delta_\Phi(w,z) = 0\,.
\end{aligned} \tag{B.25}$$

Rewriting this in terms of the four-point Green's function defined in (B.19) gives:

$$G_{lm;ij}(w,z;x,y) = G_{li}(w,x)G_{mj}(z,y) + G_{lj}(w,y)G_{mi}(z,x) \tag{B.26}$$

$$-\,2g^2\int \mathrm{d}^4a \int \mathrm{d}^4b\, G_{l\alpha}(w,a)G_{m\beta}(z,b)\Delta_\Phi(a,b)G_{\alpha,\beta;i,j}(a,b;x,y)\,. \tag{B.27}$$

This is the Bethe-Salpeter equation! By inspection, we can pick out the kernel V, the lowest order ladder diagram, as

$$V = -g^2\Delta_\Phi(a,b)\,. \tag{B.28}$$

C Tschebyshev Polynomials

For completeness we list some of the important properties of the complete set of polynomials called Tschebyshev polynomials. These polynomials are very similar in form to the well known Legendre polynomials. All of the following information can be found in various mathematical methods books such as Arfken [15].

One may obtain the Tschebyshev polynomials $T^i(x)$ from the recursion relation

$$T^{i+2}(x) = 2xT^{i+1}(x) - T^i(x) \tag{C.1}$$

and knowledge of the first two: $T^0(x) = 1$ and $T^1(x) = x$. The lowest several moments are given in Table 2.

The orthogonality of the $T^i(x)$ is given by

$$\int_{-1}^{+1} \mathrm{d}x \frac{T^i(x)T^j(x)}{\sqrt{1-x^2}} = \begin{cases} \pi & i=j=0, \\ \pi/2 & i=j\neq 0, \\ 0 & \text{otherwise.} \end{cases} \tag{C.2}$$

$T^0(x) = 1$
$T^1(x) = x$
$T^2(x) = 2x^2 - 1$
$T^3(x) = 4x^3 - 3x$
$T^4(x) = 8x^4 - 8x^2 + 1$
$T^5(x) = 16x^5 - 20x^3 + 5x$

Table 2. Tschebyshev polynomials of the first kind $T^i(x)$

D Quantizing Integrals with Gaussian Quadratures

The integral

$$I = \int_a^b f(x)\mathrm{d}x \tag{D.1}$$

can be evaluated by replacing the continuous domain with one that is finite and quantized. The method of Gaussian quadratures prescribes the set of points $\{x_i\}$, called the *mesh points*, as well as the appropriate integration weights for each point $\{W_i\}$. The sets $\{x_i\}$ and $\{W_i\}$ depend only on the endpoints of the integration domain a and b and not the particular function $f(x)$. It can be shown that if $f(x)$ is a polynomial of order m or less, the integral (D.1) satisfies

$$\int_a^b f(x)\mathrm{d}x = \sum_{i=1}^{m} F_i W_i \tag{D.2}$$

exactly! The continuous function $f(x)$ has been replaced by a vector $\vec{F}$ with

$$F_i = f(x_i). \tag{D.3}$$

It should be emphasized that the appropriateness of Gaussian quadratures for a particular problem depends on how well $f(x)$ can be approximated by a polynomial of order m. In this paper, all integrals are evaluated in this manner.

We now turn our attention to the solution of an *integral equation* numerically. The simplest example is the homogeneous integral equation

$$Y(x) = \int \mathrm{d}x' A(x,x')Y(x')\,. \tag{D.4}$$

As with the simple integration example given above, we use Gaussian quadratures to convert the integral equation into a matrix equation in an obvious generalization. The functions $Y(x)$ are replaced by $\vec{Y}$ and the kernel $A(x,x')$ is replaced by a square matrix $\mathbf{A}$. Writing the vector indices explicitly, the integral equation (D.4) becomes

$$Y(x_i) = \sum_{j=1}^{m} A(x_i,x_j)W_j Y(x_j), \tag{D.5}$$

or more compactly

$$Y_i = \sum_{j=1}^{m} A_{ij}Y_j, \tag{D.6}$$

where we have redefined A_{ij} to include the quadrature weights. In this manner, we have reduced the difficult integral equation (D.4) to an eigenvalue problem. The solution of (D.4) is approximated by the eigenvector with eigenvalue $\lambda = 1$.

E Another Look at the Democratic Method

We take this opportunity to examine the validity of the democratic method. Figure 14 shows the standard deviation of the components of the nth iterate plotted against the computed value of λ_2. We define the standard deviation as

$$\sigma(\lambda_2) = \sum_{i=1}^{N} \left(\langle \lambda_2 \rangle - \frac{Y_i^{(n)'}}{Y_i^{(n-1)'}} \right)^2 \tag{E.1}$$

where

$$\vec{Y}^{(n)\prime} = \vec{Y}^{(n)} - \lambda_1 \vec{Y}^{(n-1)} \tag{E.2}$$

is the *nth reduced iterate*, and $\langle \lambda_2 \rangle$ is the mean value of $\{\lambda_2(i)\}$ for the nth iterate. Each diamond in Figure 14 represents the calculation of λ_2 for a different iteration n. The first iterations ($n < m$) are located to the right of the dip, while the higher iterations ($n > m$), are located to the left of the dip. The democratic method prescribes that the best choice for λ_2 is that with the smallest standard deviation. From Figure 14 we observe that the values for λ_2 are clustered about the the minimum of $\sigma(\lambda_2)$.

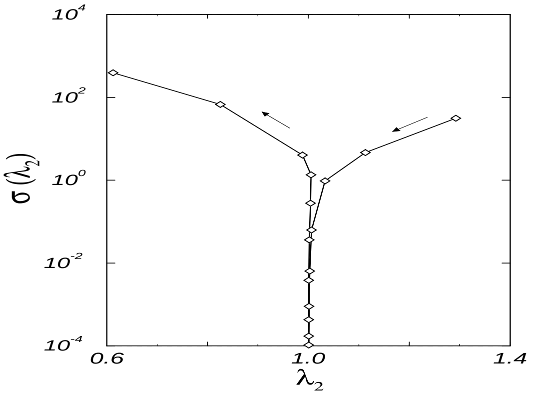

Figure 14. Deviation of λ_2 between the different components of $\vec{Y}^{(n)}$ for each n. The arrows indicate the direction of increasing interation n. The minimum shown corresponds to the "best choice" iteration m to calculate λ_2, as prescribed by the democratic method.

In order to understand why the democratic method works so well, and what its limitations are, let us write the nth reduced iterate $\vec{Y}^{(n)\prime}$, defined in (E.2), as

$$\begin{aligned} \vec{Y}^{(n)\prime} &= (\mathbf{A} - \lambda_1)\vec{Y}^{(n-1)} \\ &= \mathbf{A}^{n-1}(\mathbf{A} - \lambda_1)\vec{Y}^{(0)}. \end{aligned} \tag{E.3}$$

We see that the nth reduced iterate $\vec{Y}^{(n)\prime}$ is the vector obtained after the dependence of $\vec{X}^1$ is removed from $\vec{Y}^{(0)}$ and then multiplied by $\mathbf{A}$ n times. In an ideal world, once we have obtained λ_1, we can subtract off all of the zeroth iterates dependence on $\vec{X}^1$ and then λ_2 would be the largest eigenvalue remaining, and so we have reduced the problem to finding the largest eigenvalue again! As before we obtain the largest eigenvalue from the ratio of two successive iterations

$$\frac{\vec{Y}^{(n)\prime}}{\vec{Y}^{(n-1)\prime}} \longrightarrow \lambda_2 \tag{E.4}$$

for large enough n. This ratio is what appears in (E.1), and so we would think that

$$\lim_{n\to\infty} \sigma(\lambda_2(n)) = 0. \tag{E.5}$$

This is the justification of the democratic process. The smaller σ becomes, the closer $\vec{Y}$ comes to $\vec{X}^2$.

However, in the real world we find that this does not occur. For iterations $n > m$ (m is defined to be the iteration for which σ is minimum) we are moving to the left of the dip in Figure 14 and find that $\sigma(\lambda_2)$ is no longer going to zero but rather, it is increasing! What has happened? Roundoff errors have introduced a non-zero component of $\vec{X}^1$ into our equations and it has been growing with each iteration. As we move past the dip the components of $\vec{X}^1$ have grown enough so that once again they dominate over $\vec{X}^2$.

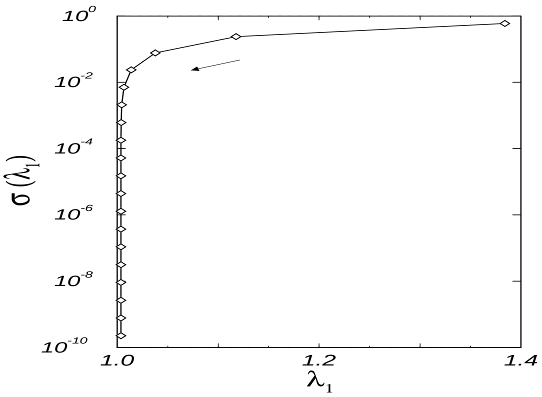

Figure 15. Same as in Figure 14 except for λ_1. In this case the "best choice" of iteration k for λ_1 is never reached. Each higher iteration gets a better value for λ_1 than the previous.

In the calculation of λ_1, we did not need to worry about $\vec{X}^1$ being overpowered by some other eigenvector since it is the largest. We expect that a similar analysis of $\sigma(\lambda_1)$ would show

$$\lim_{k\to\infty} \sigma(\lambda_1) \longrightarrow 0 \, . \tag{E.6}$$

And this is indeed the case, as shown in Figure 15. Increasing the number of iterations k will always give a more accurate value of λ_1, in sharp contrast to the previous case for λ_2.

The only restriction on the number of eigenvalues obtained in this manner is that with each new eigenvalue obtained, the "dip" which signals the location of the next becomes wider, shallower, and occurs earlier in the iterative process. At some point, the best choice of iteration for a particular eigenvalue will lie between the zeroth and first iterate. To obtain this eigenvalue would require having began the process of obtaining λ_1 with many more interations n.

References

[1] B. Ferreti, Nuovo Cimento 8, 108 (1951); K. Nishijima, Prog. Theor. Phys. 6, 37 (1951).

[2] E. E. Salpeter and H. A. Bethe, Phys. Rev. 84, 1232 (1951).

[3] G. C. Wick, Phys. Rev. 96, 1124 (1954); R. E. Cutkosky, Phys. Rev. 96, 1135 (1954).

[4] S. J. Stainsby, R. T. Cahill, Phys. Lett. A146 (1990) 467.

[5] H. Ito, W. Buck, and F. Gross, Phys. Lett. B248, 28 (1990).

[6] C. Itzykson and J.B. Zuber, *Quantum Field Theory*, 289 (McGraw–Hill Inc., 1980).

[7] K. Nishijima, *Fields and Particles*, 259 (W.A. Benjamin Inc., 1969).

[8] L. H. Ryder, *Quantum Field Theory*, p. 192,388 (Cambridge University Press, 1985).

[9] R. Woloshyn and A. Jackson, Nucl. Phys. B64, 269 (1973).

[10] V. N. Faddeeva, *Computational Methods of Linear Algebra*, p. 55 (Dover Publications Inc., 1959).

[11] F. Gross, Phys. Rev. C26, 2203 (1982).

[12] P. Jain, H. J. Munczek, Phys. Rev. D48, 5403 (1993); H. J. Munczek, P. Jain, Phys. Rev. D46, 438 (1992).

[13] F. Cooper, private communication.

[14] R. W. Haymaker, T. Matsuki, and F. Cooper, "Comparison of Alternative Effective Potentials for Dynamical Symmetry Breaking", Phys. Rev. D35, 2567 (1987).

[15] G. Arfken, *Mathematical Methods for Physicists*, p. 731 (Academic Press, Inc., 1985).